International Journal of Design & Nature and Ecodynamics
Vol. 21, No. 3, March, 2026, pp. 607-621
Journal homepage: http://iieta.org/journals/ijdne

Groundwater Drought Vulnerability in Tropical Urban Watersheds Under Climate and Land Use Change Scenarios

La Gandri[1], La Baco Sudia[1*], Kahirun[1], Davik[1], Muhsimin[1], La Ode Muhammad Firmansyah[1], Vivi Fitriani[2]

[1] Department of Environmental Science, Faculty of Forestry and Environmental Science, Halu Oleo University, Kendari 93232, Indonesia
[2] Department of Soil Science, Faculty of Agriculture, Jember University, Jember 68121, Indonesia

Corresponding Author Email: labaco.sudia@uho.ac.id

https://doi.org/10.18280/ijdne.210301

Received: 10 January 2026
Revised: 28 February 2026
Accepted: 25 March 2026
Available online: 31 March 2026

Keywords:
climate change scenario, Groundwater Drought Vulnerability Index, geospatial modelling, groundwater drought vulnerability, land use dynamics

ABSTRACT

Tropical urban watersheds are increasingly vulnerable to groundwater drought due to the combined effects of land use change, groundwater dependence, and climate variability. This study assessed current and future groundwater drought vulnerability in the Wanggu Watershed, Indonesia, using a geospatially integrated Groundwater Drought Vulnerability Index (GDVI) based on groundwater dependency, geohydrological conditions, and climatological factors. Factor weights were derived using the Analytical Hierarchy Process (AHP), while future land use and climate conditions were projected using the Geographical Simulation and Optimization System–Future Land Use Simulation (GeoSOS-FLUS) model and bias-corrected Coupled Model Intercomparison Project Phase 6 (CMIP6) scenarios under Shared Socioeconomic Pathways (SSP2-4.5 and SSP5-8.5). Results show that historical vulnerability ranges from low to very high, with most of the watershed currently classified as moderate to high vulnerability and hotspots concentrated in the south-central area. Future projections indicate a marked increase in groundwater drought vulnerability, particularly under SSP5-8.5, where high to very high vulnerability expands across much of the watershed. This increase reflects the combined influence of land use change and stronger hydroclimatic stress, especially higher evapotranspiration relative to rainfall. These findings highlight the need for spatially targeted groundwater management, including recharge area protection, groundwater abstraction control, and adaptive land use planning to strengthen long-term water security. The approach provides a practical basis for drought mitigation and future planning.

1. INTRODUCTION

Groundwater plays a crucial role in the hydrological system, serving as the largest source of freshwater, easily accessible, and widely utilized to meet human needs, ranging from domestic needs to agricultural and industrial activities [1, 2]. Groundwater is closely linked to watersheds, which constitute a unified hydrological system. Within this system, watersheds regulate the interaction between surface water flow and groundwater availability. The biophysical characteristics of watersheds significantly determine infiltration capacity and groundwater recharge processes [3, 4].

Urban development and the conversion of land to built-up areas, which frequently occur in tropical urban areas, make groundwater availability highly vulnerable. This condition can significantly impact infiltration capacity, increasing surface runoff during the rainy season, thus disrupting groundwater recharge [5, 6]. Groundwater exploitation can affect the hydrological balance of watershed areas, which supply water resources for various human needs. This, combined with rising surface temperatures, increased evapotranspiration rates, and unpredictable climate variability, will disrupt the balance between groundwater recharge and withdrawal [7, 8]. The resulting impact is a decline in groundwater levels, particularly during dry periods, which can increase vulnerability to groundwater drought, posing a risk to water security and sustainable development [9]. Recent studies from tropical regions show that groundwater systems are increasingly pressured by climate change, urban growth, and limited long-term monitoring capacity [10-12], but also by hydrogeological conditions [11-13].

Drought is a complex phenomenon that develops through several interrelated stages: meteorological, hydrological, agricultural, and socioeconomic. Meteorological drought, a condition resulting from rainfall deficit, is often considered the primary trigger of hydrological drought, affecting surface runoff, infiltration, and groundwater storage [14-17]. This meteorological drought impacts agriculture, which requires water for cultivation management, and thus impacts the socioeconomic conditions of communities [18, 19].

Several studies have used geospatial-based drought indices to assess drought conditions, such as the use of the

standardized precipitation index (SPI) and standardized precipitation evapotranspiratin Index (SPEI) indices for monitoring meteorological drought and its impacts [20-22], the use of the Soil Moisture Index (SMI) for evaluating agricultural drought [23, 24], and hydrological drought evaluation using the Stream Flow Index [25-28].

A recent study in a tropical region in Indonesia used SPI to assess meteorological drought, especially in Jember Regency [29], and a recent review in tropical Southeast Asia also found that the assessment of drought in this region is still dominated by SPI, SPEI, and Palmer drought severity index (PDSI), while important gaps remain in index sensitivity and climate-related applications [12]. This shows that most of these studies focus on monitoring and evaluating meteorological and surface-water drought vulnerability, especially in tropical regions, even though recent evidence shows that drought propagation can vary by climate and may not be controlled by precipitation alone [30], while groundwater drought vulnerability remains relatively underexplored.

Moreover, groundwater drought assessments are commonly limited to historical conditions, with little attention paid to future climate projections and land-use dynamics. This gap is especially critical in tropical urban watersheds, where groundwater abstraction, land conversion, and climate-driven changes in evapotranspiration interact in complex ways. Integrated assessments that combine groundwater dependence, geohydrological characteristics, climate change, and land use change are still scarce, particularly in tropical urban watersheds [10, 11, 30].

The Wanggu Watershed, located in Southeast Sulawesi, Indonesia, represents a typical tropical urban watershed experiencing increasing hydrological stress, based on previous studies [31, 32], declining infiltration capacity, expanding built-up areas, and intensified groundwater exploitation within the watershed, which may result in high potential vulnerability to drought even in the future.

In response to these challenges, this study addresses that gap by applying a geospatially integrated Groundwater Drought Vulnerability Index (GDVI) to assess current and future groundwater drought vulnerability under changing climate and land use conditions. This research can provide a comprehensive assessment framework to support sustainable groundwater management and enhance resilience in tropical urban watersheds under increasing hydroclimatic pressure.

2. RESEARCH METHOD

The Wanggu watershed, located in Southeast Sulawesi, Indonesia, covers three regions: the South Konawe District, the Konawe District, and Kendari City, with geographic coordinates ranging from 3°59′23″ S – 4°10′14″ S and 122°22′26″ E – 122°33′14″ E (Figure 1).

2.1 Groundwater drought vulnerability

A groundwater drought vulnerability assessment was conducted using the method proposed by Ling et al. [14] and the GDVI algorithm. This index is a measure of groundwater drought vulnerability, a composite of various variables that influence the potential for groundwater to experience drought. The assessment of dependence on groundwater, geohydrological conditions, and climatological conditions is the three main variables to be evaluated. Drought vulnerability assessment was done for two time frames: current or historical conditions and future scenarios. The assessments over two different periods were conducted to identify current potential drought vulnerability and project future drought risks, which are used as a form of anticipation. This assessment will provide a basis for sustainable groundwater management as a form of adaptation and mitigation of drought hazards.

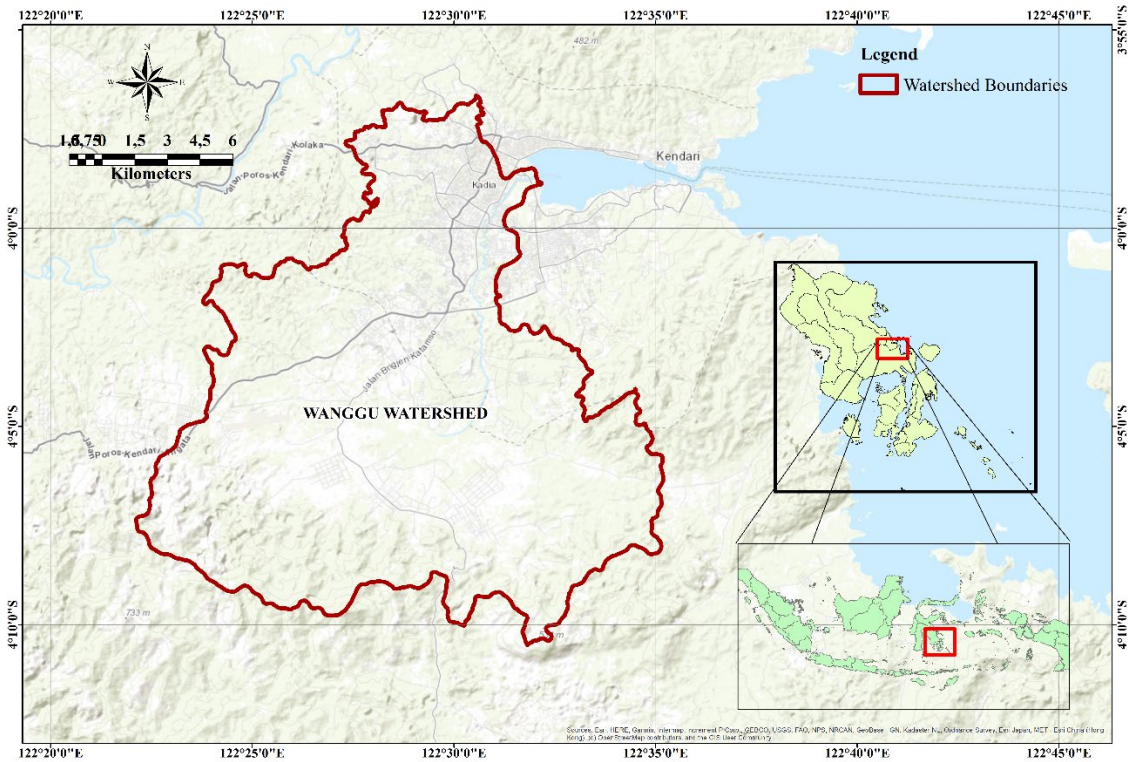

Figure 1. The Wanggu watershed

2.1.1 Groundwater dependency

Groundwater dependency refers to the extent to which local populations and economic activities rely on groundwater resources for domestic, agricultural, and industrial needs. In the study area, groundwater dependency was assessed through three indicators, which consist of (1) groundwater exploitation, (2) distance to surface water, and (3) land use. First, groundwater exploitation was assessed as the direct use of groundwater for human needs, particularly domestic consumption, with data obtained through field surveys and structured interviews. The exploitation value was determined based on the ratio between actual water use for household needs and the standard water requirement based on Permendagri No. 23 [33]. Second, the distance to surface water was calculated using buffer analysis of river networks with Geographic Information System (GIS) software to determine the accessibility of alternative water sources. Third, land use was derived from the acquisition and analysis of LANDSAT 8/9 OLI TIRS satellite imagery for the period 2015–2024, processed through the Google Earth Engine (GEE) platform and classified using the supervised classification method in GIS software to capture spatial patterns of land cover affecting groundwater dependency.

2.1.2 Geohydrological condition

There are four main variables used to determine the geohydrological conditions of the soil that influence the vulnerability of groundwater to drought: groundwater potential, shallow well depth, permeability, and slope gradient. Groundwater depth is obtained from well measurements at several sampling points; permeability is calculated from laboratory analyses of soil samples; and slope gradient is derived from remote sensing data, specifically a digital elevation model (DEM). Geohydrological conditions indicate the soil's ability to store water in the soil layer through runoff and recharge processes.

2.1.3 Climatological condition

Assessment of Climatological Conditions in Influencing the Vulnerability of Groundwater Drought in the Wanggu Watershed using the two main variables, namely rainfall and Evapotranspiration. Rainfall data were analyzed over 10 years from 2013 to 2024 in the form of an annual average. To calculate Evapotranspiration, the Hargreaves-Samani method was used based on air temperature data for 10 years in the form of maximum, minimum, and average temperatures [34, 35]. This Climate Data was obtained from BMKG, which was used to determine how water availability in the soil is affected by the difference between rainfall values and evapotranspiration values.

2.2 Groundwater Drought Vulnerability Index

The indicator used to assess the vulnerability of groundwater drought in the Wanggu Watershed is the GDVI developed by Ling et al. [14]. GDVI is a measure that takes into account the factors that have the most significant impact on the groundwater drought situation. The computation of GDVI in this paper is based on the location where the variables are considered as spatial data.

To determine the relative influence of each variable, factor weights were derived using the Analytical Hierarchy Process (AHP) based on expert pairwise comparisons conducted in Expert Choice software [14, 36-38]. The assessment involved five experts representing the fields of hydrology, climatology, watershed management, and relevant technical agencies. In this procedure, the evaluation criteria were first structured hierarchically, after which pairwise comparisons were performed to derive normalized priority weights for each variable.

The consistency of expert judgments was evaluated using the Consistency Index (CI) and Consistency Ratio (CR) [14, 37] as expressed in Eqs. (1) and (2), where the pairwise comparison matrix was considered acceptable when CR < 0.10.

$$CI = (\lambda_{max} - n)/(n-1) \quad (1)$$

$$CR = CI/RI \quad (2)$$

where, λ_{max} is the maximum eigenvalue, n is the order of the comparison matrix, and RI is the Random index.

The GDVI was calculated using the weighted linear combination using the following Eq. (3).

$$\text{GDVI} = \sum_{i=1}^{n} W_i X_i \quad (3)$$

where W_i is the weight of the i-th parameter, and X_i is the score of the i-th parameter.

Each geospatial factor that affects the GDVI has different magnitudes and units. Hence, to make the values and units equivalent, they are standardized first before using Eq. (1). The standardization process is done by the calculations illustrated in Eqs. (4.1) and (4.2). The use of these equations is based on the relationship between geospatial variables and groundwater drought vulnerability. If the geospatial variables have a positive correlation, Eq. (4.1) is used. If the geospatial variables have a negative correlation, then the standardization process uses Eq. (4.2) [14].

$$X_i = 10(y_{max}-y_i)/(y_{max}-y_{min}) \quad (4.1)$$

$$X_i = 10(y_i-y_{min})/(y_{max}-y_{min}) \quad (4.2)$$

where X_i is the standardized value of the factors influencing vulnerability, y_i is the original value of the i-th factor, y_{max} is the maximum value of the i-th factor, and y_{min} is the minimum value of the i-th factor. For categorical factors such as land use, the scoring is based on scientific references by Yuan et al. [39], which were then modified by the researchers to accommodate the number of land uses in the study area.

From the standardization process, the resulting GDVI ranges from 0 to 10. This index range is used to categorize groundwater drought vulnerability. An index value < 2 indicates very low vulnerability, 2-4 indicates low vulnerability, 4-6 indicates moderate vulnerability, 6-8 indicates high vulnerability, and an index value > 8 indicates very high drought vulnerability [14].

2.3 Future projection of groundwater drought vulnerability

The assessment of future groundwater drought vulnerability uses the same geospatial factors as the existing vulnerability factors. However, three factors are projected for future vulnerability assessment: land use, rainfall, and evapotranspiration. These three factors are projected for the period 2025 to 2050.

2.4 Land use projection

Future land use projections are conducted by integrating geographic information systems and the GeoSOS-FLUS model [40]. The 2019 land-use map was used as the initial land-use map, while the 2025 land-use map was used as the observed reference map for model validation. Before simulation, all raster inputs were standardized to the same rows and columns, and land-use classes were reclassified into consecutive integer codes. The model incorporated several driving factors, including distance to settlements, roads, airports, and health facilities, as well as population density, topography, and historical rainfall. Land-use change was simulated using two main modules in GeoSOS-FLUS, namely Artificial Neural Network (ANN)-based Probability-of-occurrence Estimation and Self-Adaptive Inertia and Competition Mechanism CA. Model performance was evaluated using the Kappa Statistic Tool by comparing the simulated 2025 land-use map with the observed 2025 land-use map. After the model performance was confirmed, future land-use demand was projected using the Markov Chain Model. The Kappa coefficient is a statistical validation metric which used to assess the model's ability to predict land use. If the Kappa value is > 0.80, it reflects the model's strong performance, reliability, and good spatial prediction accuracy between simulated and observed [41, 42]. However, the GeoSOS-FLUS simulation is still subject to uncertainty related to the selection of driving factors, the calibration of the ANN module, the transition settings in the CA module, and the quality of the historical land-use maps used for training and validation. Therefore, the projected land-use pattern should be interpreted as a plausible future scenario rather than an exact spatial prediction.

2.5 Climate projection and bias correction

Climate projections are vital for the command and control to get the gist of the environmental risks caused by climate change and to lay down the scientific basis for the long-run strategies of mitigation and adaptation [43, 44]. Various General Circulation Models (GCMs) have been employed to depict the changes caused by the global climate crisis over different environmental systems. In this research, the selected GCMs from the Coupled Model Intercomparison Project Phase 6 (CMIP6), which is a source of coordinated climate simulations from multiple models, are used, thus giving more data for climate impact assessments [45, 46].

Specifically, two CMIP6 models, Centro Euro-Mediterraneo on Climate Change Earth System Model version 2 (CMCC-ESM2) and Australian Community Climate and Earth-System Simulator – Climate Model version 2 (ACCESS-CM2), were selected based not only on the availability of key climate variables (precipitation and maximum–minimum air temperature) but also on their documented ability to represent large-scale climate variability in regions [47, 48]. These models have been widely used in previous climate impact studies and provide consistent outputs required for hydrological assessments. The datasets were obtained through the CMIP6 Earth System Grid Federation (ESGF) data portal. The datasets were obtained through the CMIP6 ESGF data portal (https://esgf-node.ipsl.upmc.fr/search/cmip6-ipsl/). Three periods were considered: (1) the historical period, which served as the baseline for 2013-2024, and (2) two future Shared Socioeconomic Pathways (SSP2-4.5 and SSP5-8.5) for the 2025-2050 period, representing intermediate and high greenhouse gas emission scenarios, respectively [49-51] The selection of these two scenarios aims to evaluate the range of possible future hydrometeorological conditions, from moderate to extreme, that could potentially impact groundwater dynamics in the Wanggu Watershed.

However, GCMs operate at coarse spatial resolutions and are often unable to capture local topographic variations and small-scale climatic processes accurately. Then, to better represent local climatic conditions in the study area, the selected CMIP6 outputs were bias-corrected using the Delta Change Method, a commonly applied approach for downscaling and adjusting GCM outputs to match local observations [45, 52-54]. Observational data from a local climatological station were used as the reference for bias correction, ensuring that the adjusted datasets reflect both the observed historical climate and the projected climate change signal at the local scale. Due to the incompleteness of ground-based observations, this study employed the fifth-generation ECMWF reanalysis (ERA5)-Land reanalysis data for the minimum and maximum air temperature [55] and CHIRPS satellite-based precipitation data [56] as secondary datasets to support spatial and temporal calibration. The ERA5-Land and CHIRPS datasets were calibrated against observation data to enhance spatial coverage and temporal consistency across the study area [57]. The entire data processing and analysis workflow was conducted using GEE and RStudio to ensure reproducibility and computational efficiency.

Specifically, ERA5-Land temperature data were calibrated using observed maximum and minimum air temperatures using Eq. (5), and subsequently used to estimate reference evapotranspiration (ET_0) using the Hargreaves–Samani method [35, 58], as expressed in the following formula:

$$ET_{0,HS} = 0.0023\, R_a\, (T_{max} - T_{min})^{0.5}(T_a + 17.8) \qquad (5)$$

where ET_0 is the reference evapotranspiration (mm day^{-1}), Ta is the mean air temperature (°C), T_{max} and T_{min} are the daily maximum and minimum temperatures (°C), R_a is the extraterrestrial radiation based on the latitude position of the study area, and 0.0023 is an empirical coefficient

The empirical coefficient of the Hargreaves–Samani equation was locally calibrated to represent site-specific climatic conditions. The calibrated ERA5 dataset was then used as a reference for bias correction of GCM temperature data.

For precipitation, CHIRPS data were first calibrated against observed rainfall using a monthly scaling approach. The calibrated CHIRPS dataset was then used as the reference for bias correction of GCM precipitation data using a multiplicative scaling method. This two-stage bias correction framework ensures that both satellite-based and model-derived precipitation data are consistent with local observational conditions.

The bias correction functions derived from the baseline period were subsequently applied to future climate scenarios (SSP2-4.5 and SSP5-8.5), ensuring temporal consistency in the correction process. Although the bias-correction procedure improves the consistency of CMIP6 outputs with local observations, residual uncertainty remains because coarse-resolution climate models may not fully represent watershed-scale climatic heterogeneity, especially for rainfall and evapotranspiration. Therefore, the corrected projections

should be interpreted as scenario-based estimates rather than exact local predictions [59-61].

The Delta Change Method adjusts GCM projections by applying the modeled future change signal (delta) to the observed baseline [52, 54, 62, 63]. The downscaling process for precipitation and temperature data is expressed by the following formula [14, 64]:

$$P_f = P_0 \, (P_{Gf} / P_{G0}) \quad (6)$$

$$T_f = T_0 + (T_{Gf} - T_{G0}) \quad (7)$$

where, P_f and T_f are the bias-corrected future precipitation and temperature, respectively, P_0 and T_0 are observation baseline values for precipitation and temperature, respectively. P_{G0} and T_{G0} represent the historical GCM simulations for precipitation and temperature, respectively, and P_{Gf} and T_{Gf} represent the future GCM simulations for precipitation and temperature, respectively.

3. RESULT AND DISCUSSION

3.1 Groundwater drought vulnerability factors assessment (historical period)

The assessment of groundwater drought vulnerability was carried out using the GDVI approach. The GDVI calculation is based on three main variables: groundwater dependency, geohydrological conditions, and climatological conditions. A total of nine parameters were evaluated according to the characteristics of the study area, namely: groundwater exploitation, distance to surface water, land use, groundwater potential, shallow well depth, permeability, slope, precipitation, and evapotranspiration.

3.1.1 Groundwater dependency

One of the factors that influences groundwater drought vulnerability is groundwater dependence. Groundwater dependence reflects the relationship between human groundwater use and groundwater availability. The spatial distribution of groundwater dependence in the Wanggu watershed, based on distance to surface water, groundwater exploitation, and land use, is shown in Figure 2 and Table 1.

Table 1. Areal statistics of groundwater dependency factors

Parameter	Class	Area (ha)	Percentage (%)
Distance to surface water	<100 m	15,583.19	46.4
	100–500 m	15,701.55	46.8
	500–1000 m	2,088.25	6.2
	>1000 m	210.23	0.6
Groundwater exploitation	Very good	1,325.50	3.9
	Good	6,882.66	20.5
	Medium	12,798.74	38.1
	Bad	5,303.09	15.8
	Very bad	7,273.24	21.7
Land use	Built-up land	5,520.41	16.4
	Forest	13,827.74	41.2
	Agriculture	4,170.99	12.4
	Open land	1,211.84	3.6
	Scrub	8,717.43	26.0
	Pond	68.46	0.2
	Mangrove	19.15	0.1
	Water body	47.19	0.1

Source: data analysis, 2026

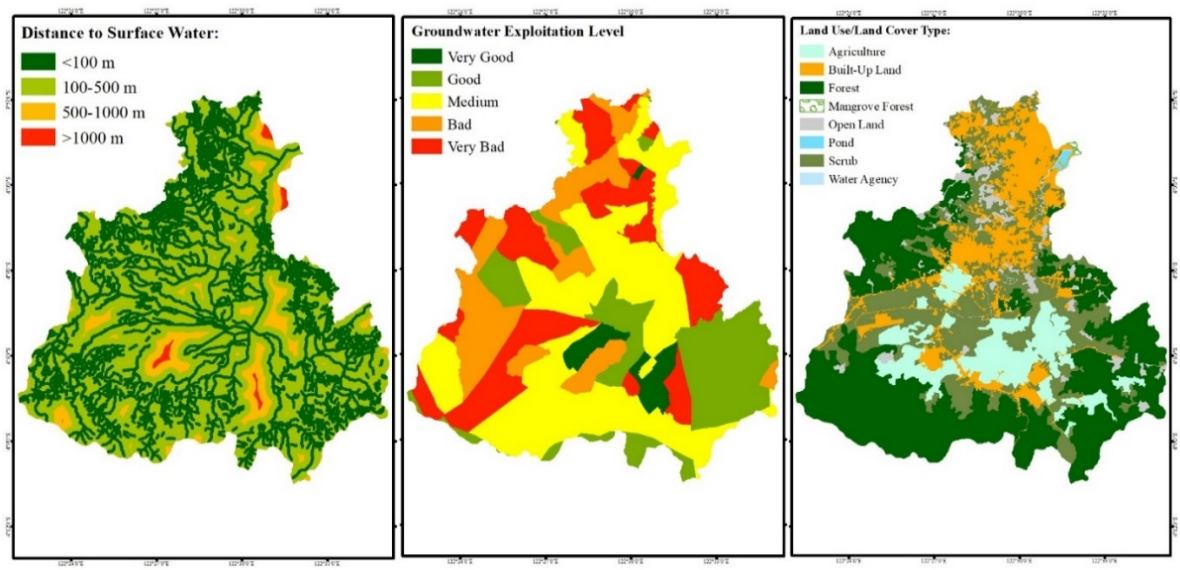

Figure 2. Groundwater dependency factors: (a) distance to surface water, (b) groundwater exploitation level, (c) land use

Figure 2(a) and Table 1 show that most of the watershed is located close to surface water. The < 100 m and 100-500 m classes account for 46.4% and 46.8% of the total area, respectively, while the 500-1000 m and >1000 m classes cover only 6.2% and 0.6%. Areas with the closest distance to surface water indicate that they can maintain groundwater moisture. Meanwhile, areas far from surface water will struggle to maintain groundwater moisture. This condition demonstrates the interconnectedness between surface hydrology and groundwater. This finding is in accordance with the results of research in the San Pedro River area, where a closer distance to surface water is associated with greater groundwater depth, indicating a relationship between surface water and groundwater [65, 66].

The level of groundwater exploitation, as shown in Figure 2(b) in this study, was determined based on the comparison value between domestic groundwater use and the national groundwater use standards set by the Minister of Home Affairs

Regulation No. 23, 2006 [33]. The results indicate that the watershed is dominated by medium to very bad exploitation levels. The medium class accounts for the largest proportion (38.1%), followed by very bad (21.7%), good (20.5%), bad (15.8%), and very good (3.9%). Areas with high levels of exploitation are concentrated in the north-central region. Naturally, groundwater exploitation is driven by increasing population growth, which in turn increases groundwater extraction. In addition, the development of groundwater extraction technologies, such as well drilling, water pumps, and rural electrification, provides easy access to groundwater extraction [67]. As observed in the San Pedro River, the phenomenon of excessive groundwater extraction through intensive local pumping has caused a decline in the groundwater table [68]. This condition indicates that excessive extraction can lower the groundwater table and deplete aquifers, increasing the potential for groundwater drought.

The next factor influencing groundwater dependence is land use, which indicates anthropogenic pressure on the surface hydrological cycle. Based on Figure 2(c) and Table 1, the Wanggu watershed is dominated by forest, which covers 41.2% of the total area, followed by scrub (26.0%), built-up land (16.4%), and agriculture (12.4%). According to the study [69], one factor influencing the groundwater hydrological system is land use. Land cover and land use significantly influence the amount of infiltrated water flow, thus affecting groundwater recharge and water use for domestic and agricultural purposes. Previous studies in Bantul Regency have shown that urban expansion has increased the risk of groundwater drought due to reduced infiltration and increased water demand [70]. In Kolar District, southern India, it also shows how the expansion of agricultural areas can increase the need for irrigation water by around 145% [71]. This condition may reduce the availability of groundwater during the dry season when irrigation demand is high, while groundwater recharge is at a minimum.

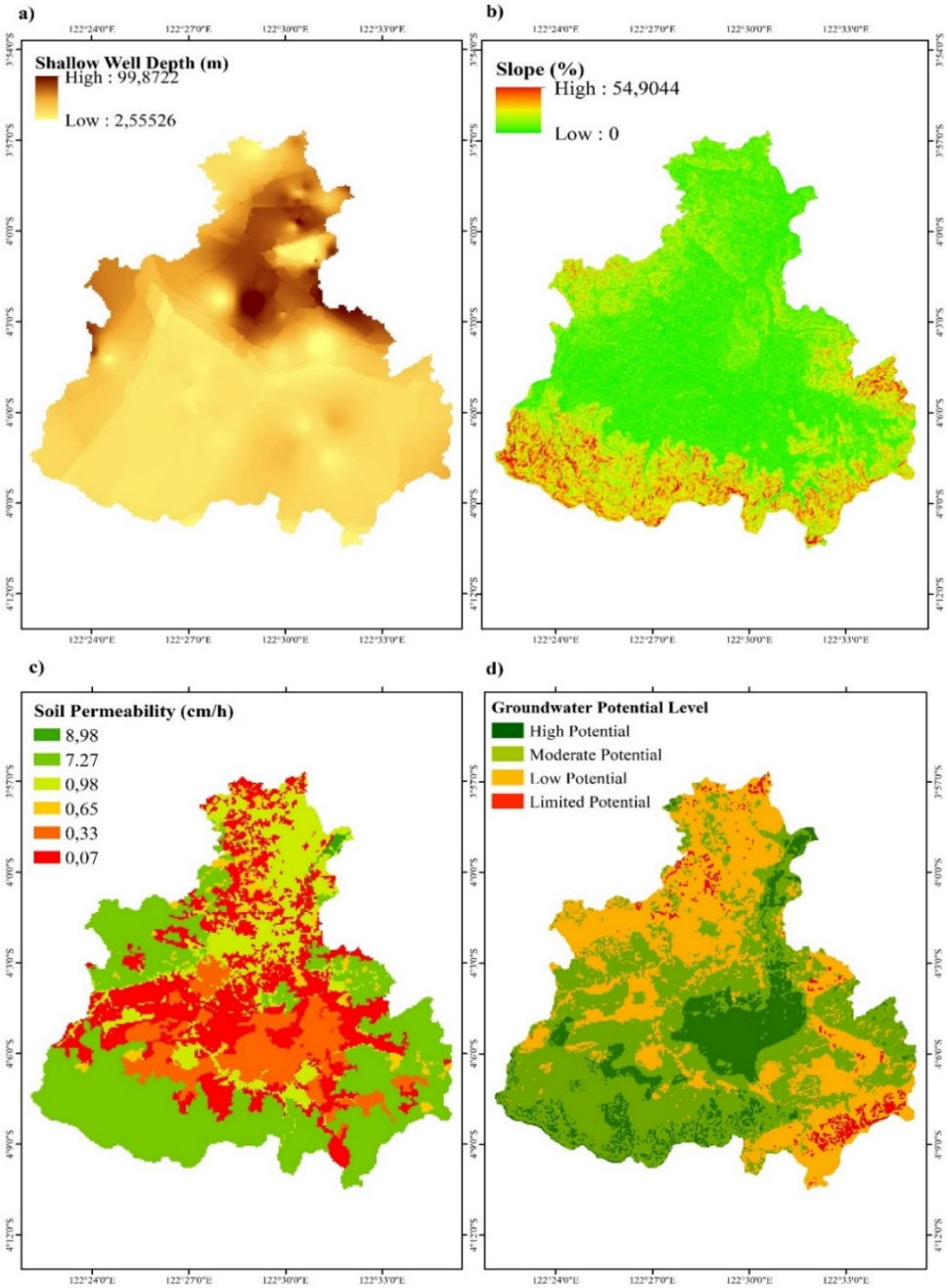

Figure 3. Geohydrological condition factors: (a) shallow well depth, (b) slope, (c) soil permeability, (d) groundwater potential level

3.1.2 Geohydrological condition

As displayed in Figure 3(a), the Wanggu watershed water tables vary in depth between 2.56 m and 99.57 m. This particular parameter suggests the position of the phreatic surface, which is considered one of the most important indicators of groundwater for domestic and agricultural purposes [72]. Areas that have shallow groundwater tables usually provide that water extraction is easier and requires less energy, while deeper water tables indicate less accessibility and greater energy pumping.

Figure 3(b) shows SSP5-8.5 scenarios. Slopes with gradients that are between 0% and 54.9%, where gentle slopes (0-8%) are predominantly found across most of the watershed, while only a small portion contains slopes greater than 25%. Slopes are one of the factors that affect the rates of runoff and infiltration. The gentle slopes help recharge the saturated zone, while steeper slopes cause runoff to increase with little or no infiltration [73]. The soil permeability map (Figure 3(c)) shows that soil permeability ranges from 0.07 to 8.98 cm/ hour. Most of the area, particularly in central regions and the surrounding areas, has low permeability. This shows how fast a particular soil type can allow water to percolate. Sandy soils tend to have a high water infiltration rate, which classifies them as fast-permeable. Clay, on the other hand, is slower-permeable and can impede water infiltration, causing high runoff rates [74].

The groundwater potential level (Figure 3(d)) indicates moderate potential across most of the Wanggu watershed. It is graded into four classes: high potential, moderate potential, low potential, and limited potential. Moderate potential means that water is indeed present underground. It may be seasonally variable or depleted seasonally [74]. It may be available and sporadically flow. Hence, recharge rate and variable groundwater depletion may be weakened or strengthened by seasonality, by one or a combination of the determinants described above. An area of high depth to water table value, high topographic slopes, low permeable soil materials, followed by low potential, may be stressed by high recharge depletion. Thus, relative water availability may increase the drought risk to the watershed. The determinants described include depth to water table value, topographic slopes, soil permeability, and potential.

3.1.3 Climatological conditions

The patterns of Evapotranspiration and precipitation in the region have high variability (Figure 4(a)–(b)). From the Evapotranspiration maps (Figure 4(a)), there is high variability in Evapotranspiration rates, ranging between 1,035.19 mm/year and 1,337.29 mm/year. The maps display a high gradient of Evapotranspiration rates from east to west. In the eastern part of the watersheds, there is a high Evapotranspiration rate. On the other hand, the western part of the watersheds indicates a low Evapotranspiration rate. Groundwater Evapotranspiration is a critical component of the hydrological cycle. Estimating the amount of Evapotranspiration in groundwater is critical in arid watersheds [75].

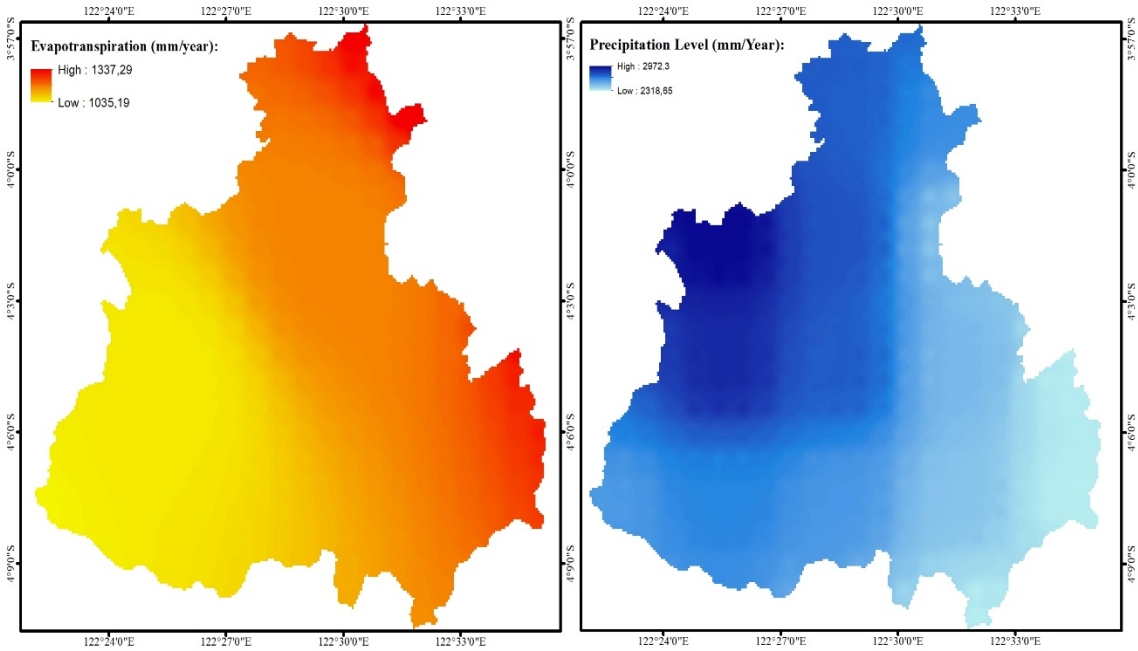

Figure 4. Climatological condition factors: (a) evapotranspiration (mm/year), (b) precipitation (mm/year)

High water utilization in the Wanggu watershed can lead to a situation where water is lost from the ground by evaporation. Similarly, this breathing process that happens in the vegetation is also slowly reduced by Evapotranspiration. The distribution of precipitation per year, as shown in Figure 4(b), reveals that the measurements of precipitation vary between 2,318.65 mm/year and 2,973.30 mm/year. The precipitation in the northern part of the catchment is very high and gradually decreases towards the southern and eastern parts. An analysis of the total precipitation in the Wanggu Watershed indicates that it is categorized as a medium area according to the BMKG classification [76]. Understanding this classification is essential for the hydroclimatic setting of the basin. It means that the basin receives moderate levels of precipitation per year. The average value of the yearly evapotranspiration is 1,186.24 mm/year. The average yearly precipitation is 2,645.98 mm/year. The huge difference between these two climatic factors shows that the water flux amount that comes from precipitation is much higher than the water flux amount that is lost to the atmosphere during the process of evapotranspiration.

This is the reason why water levels are so high, with the potential to recharge large volumes of underground water and create high surface runoff.

3.2 Groundwater drought vulnerability conditions

Groundwater drought vulnerability in the Wanggu Watershed is mainly controlled by groundwater dependence, geohydrological conditions, and climatological factors. Parameter weights, as shown in Table 2, were derived using the AHP based on pairwise comparisons from five experts in hydrology, climatology, watershed management, and relevant technical agencies. The pairwise comparison matrix met the AHP consistency requirement (CR = 0.05), indicating that the weights were derived from consistent expert judgment. The results show that precipitation, land use, groundwater potential, and evapotranspiration were the most influential parameters. This pattern is generally consistent with Ling et al. [14], who also identified land use and meteorological factors as the dominant controls in groundwater drought vulnerability assessment [14].

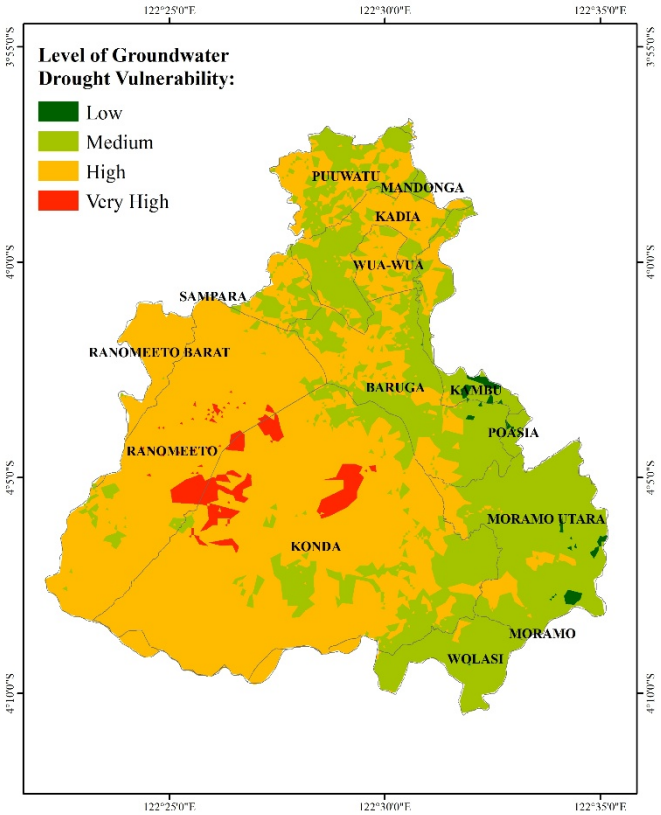

Figure 5. Groundwater drought vulnerability in the historical period

The groundwater vulnerability of the Wanggu watershed is illustrated in Figure 5. The vulnerability degree ranged from low to very high. Over the recent period, the watershed was predominantly classified as moderately to highly vulnerable.

The south-central part of the watershed, particularly West Ranomeeto, Sampara, Ranomeeto, and much of Konda, forms the main hotspot of high to very high vulnerability. In contrast, the northern and eastern areas are dominated by moderate vulnerability, while parts of Moramo and Wolasi exhibit relatively low vulnerability. This spatial pattern suggests that groundwater drought vulnerability is shaped by the interaction of anthropogenic pressure, geohydrological conditions, and hydroclimatic stress. Areas with higher vulnerability are generally associated with stronger groundwater abstraction, greater distance from surface water sources, deeper shallow wells, steeper slopes, higher evapotranspiration, and lower effective rainfall, all of which reduce recharge and increase groundwater stress. By comparison, less vulnerable areas tend to have relatively better groundwater potential and more favorable recharge conditions. These findings indicate that the south-central part of the watershed should be prioritized for groundwater abstraction control, protection of recharge areas, and intensified groundwater monitoring, whereas the moderately vulnerable areas require preventive management to avoid further deterioration.

Table 2. Results of the factor weighting assessment

Factor	Weights
Groundwater dependency	
Groundwater exploitation	0.066
Distance to surface water	0.047
Land use	0.187
Geohydrological conditions	
Groundwater potential	0.136
Shallow well depth	0.098
Soil permeability	0.071
Slope	0.050
Climatological conditions	
Precipitation	0.213
Evapotranspiration	0.133

Source: data analysis, 2025

The GDVI classes in this study should be interpreted as relative groundwater drought vulnerability categories rather than directly validated measures of drought occurrence, because the present study did not include formal validation against historical drought events, standardized drought indices, or long-term independent groundwater observations. The GDVI means the area with high to very high indicates that the area has high potential to experience drought. But it is necessary that Future studies are needed to test the robustness of the classification using independent observational and drought-related datasets.

Overexploitation of groundwater is a major factor increasing the risk of drought, particularly when the rate of extraction exceeds the rate of recharge, leading to a groundwater balance deficit. This condition increases the vulnerability of aquifer systems to hydrological stress during dry periods, as reported in global studies on groundwater depletion due to intensive extraction [77, 78]. Furthermore, distance to surface water bodies affects recharge capacity, so areas farther from surface water sources tend to have lower storage capacity and are more vulnerable to drought [79]. Shallow well systems are also more sensitive to groundwater level fluctuations, potentially experiencing decreased discharge during periods of drought or intensive extraction. In a mitigation context, increasing well depth can be one strategy to reduce water deficits [80].

Steep slopes increase surface runoff and reduce water retention and infiltration, thus limiting aquifer recharge, particularly in upland areas. This impact is even more significant in areas with high evaporation potential and low rainfall, which exacerbates water deficits during dry [81]. Conversely, areas with high groundwater potential, characterized by large aquifer capacity and good soil permeability, can serve as natural buffers during droughts [82].

High rainfall also directly contributes to increased aquifer recharge, as confirmed by GRACE satellite analysis [77].

Overall, the combination of anthropogenic and natural factors significantly shapes groundwater drought vulnerability patterns. Areas with high groundwater abstraction, high slope gradients, long distances from rivers, low permeability, high evapotranspiration, and low rainfall can be identified as priority management zones. These findings are consistent with studies in other tropical regions that emphasize the interplay of natural and anthropogenic factors in shaping groundwater drought. The implications of this research are important for formulating mitigation and adaptation strategies in the tropical watershed, particularly in assessing the region's capacity to maintain groundwater supplies during prolonged dry periods. Furthermore, these results support efforts to strengthen the watershed's function as a provider of freshwater ecosystem services [14, 39, 83].

From a practical perspective, however, the implementation of mitigation strategies must also consider local land-use planning, institutional coordination, financial capacity, and community acceptance, because groundwater recharge management is closely linked to landscape use and spatial planning decisions [84]. In densely built areas, the creation of additional green space or large recharge zones may be difficult to implement, so more feasible options may include controlling groundwater abstraction, protecting the remaining recharge areas, and introducing small-scale infiltration measures adapted to local hydrogeological conditions [85]. In areas where land conversion pressure is lower, vegetation restoration and land protection may be more realistically applied as longer-term strategies to maintain recharge capacity [84, 86]. Accordingly, groundwater management should be implemented in phases and supported by community partnerships, local regulations, and policy-based incentives to improve feasibility and long-term effectiveness [85, 86].

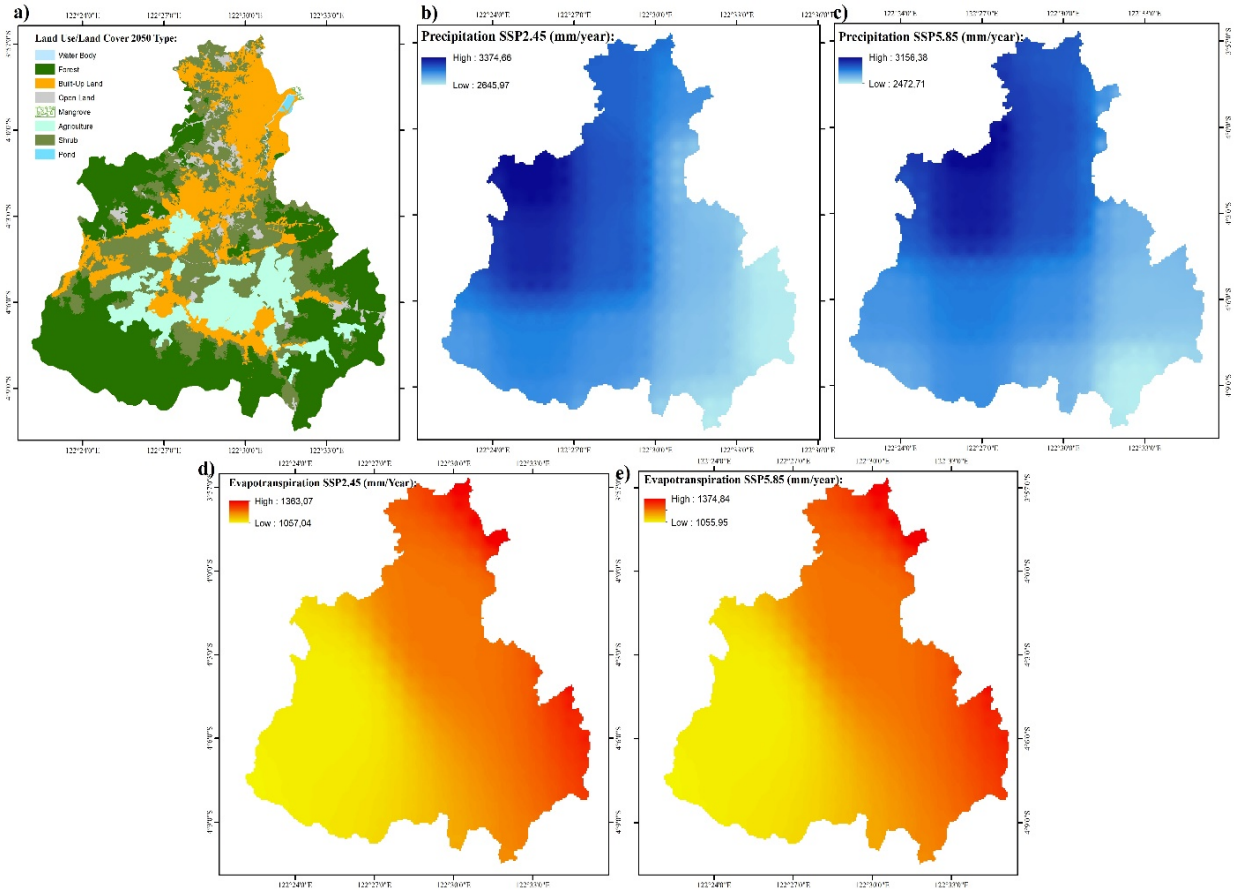

Figure 6. Projection groundwater drought vulnerability factors: (a) land use 2050, (b) precipitation at Shared Socioeconomic Pathways (SSP2-4.5) scenario, (c) precipitation at Shared Socioeconomic Pathways (SSP5-8.5) scenario, (d) evapotranspiration at Shared Socioeconomic Pathways (SSP2-4.5) scenario, (e) evapotranspiration at Shared Socioeconomic Pathways (SSP5-8.5) scenario

3.3 Projection of groundwater drought vulnerability factors assessment

3.3.1 Land use projection

Projections for land cover in 2050 were conducted using GeoFlus as shown in Figure 6(a), resulting in an overall Kappa value of 89.74%. Changes in land cover area from 2025 to 2050 are shown in Table 3. A significant increase in pond land use (331.36%), indicating very rapid expansion, and built-up land (18.19%), indicating continued urban growth, was observed. Significant decreases were found in open land (23%) and scrub (7.55%), indicating substantial land conversion. Forests decreased by 1%, indicating a continuous decline.

The increase in built-up land has the potential to be the main cause of reduced groundwater availability in the future, as the expansion of built-up areas reduces rainwater infiltration areas because built-up land materials are impermeable, thereby decreasing the ability of rainwater to infiltrate into the soil, accelerating surface runoff, reducing baseflow, and thus inhibiting groundwater recharge to the aquifer [87]. In addition,

the increasing demand for water for domestic and industrial consumption in built-up areas intensifies groundwater extraction activities, which can contribute to a decline in groundwater levels. The increase in agricultural areas is also one factor contributing to the decline in groundwater levels, as found in the Breede Water Areas, where the expansion of agricultural land can trigger increased water use for irrigation through abstraction for intensive agricultural water supply, especially during dry periods, which can cause groundwater to become vulnerable to dry conditions [88]. The reduction in open areas, shrubs, and forests can lead to the loss of natural infiltration areas that function to support aquifer recharge.

Table 3. Land use change for the 2025-2050 period

No.	Land Use	Area (ha)			%
		2025	2050	Δ	
1	Forest	14,062.43	13,921.79	-140.64	-1.00
2	Built-Up Land	5,560.22	6,571.38	1,011.17	+18.19
3	Agriculture	4,170.99	4,313.97	142.98	+3.43
4	Open Land	1,225.70	943.77	-281.93	-23.00
5	Scrub	8,786.37	8,123.38	-662.99	-7.55
5	Pond	71.59	308.82	237.23	+331.36
6	Mangrove	26.08	27.50	1.42	+5.46
7	Water Body	47.45	47.86	0.42	+0.87

Note: Where a negative sign (-) denotes a decrease in area and a positive sign (+) denotes an increase in area

3.3.2 Climate scenarios

The distribution of rainfall in the SSP2-4.5 scenario in Figure 6(b) shows a range of 2645.97-3374.66 mm/year with a high concentration in the northern region. However, in the SSP5-8.5 scenario in Figure 6(c), there is a decrease in rainfall to 2472.71-3156.38 mm/year with a maximum difference of 218.28 mm/year, especially in the northern region. As shown in Figure 6(d) and Figure 6(e), evapotranspiration under the SSP5-8.5 scenario increases compared to the SSP2-4.5 scenario, with a maximum increase of 11.77 mm/yeard. The combination of decreased rainfall and increased evapotranspiration increases the water deficit and increases the risk of drought, especially in the northern region, which also experiences land use pressure. In contrast, the southern region, which is still dominated by forests, is relatively more resilient to hydrological pressures, although land degradation still has the potential to reduce the level of resilience if not managed sustainably.

3.4 Projection of groundwater drought vulnerability

The GDVI projection in the Wanggu watershed was done using the Historical GDVI parameters derived from previous analyses. The projection model considers land use change projected for the year 2050, as well as climatological variables such as precipitation and evapotranspiration estimated over a period from 2025 to 2050. This analysis considers both land use change that is projected for the year 2050 and climate change, which together have the potential to alter the hydrological balance and groundwater recharge dynamics within the watershed.

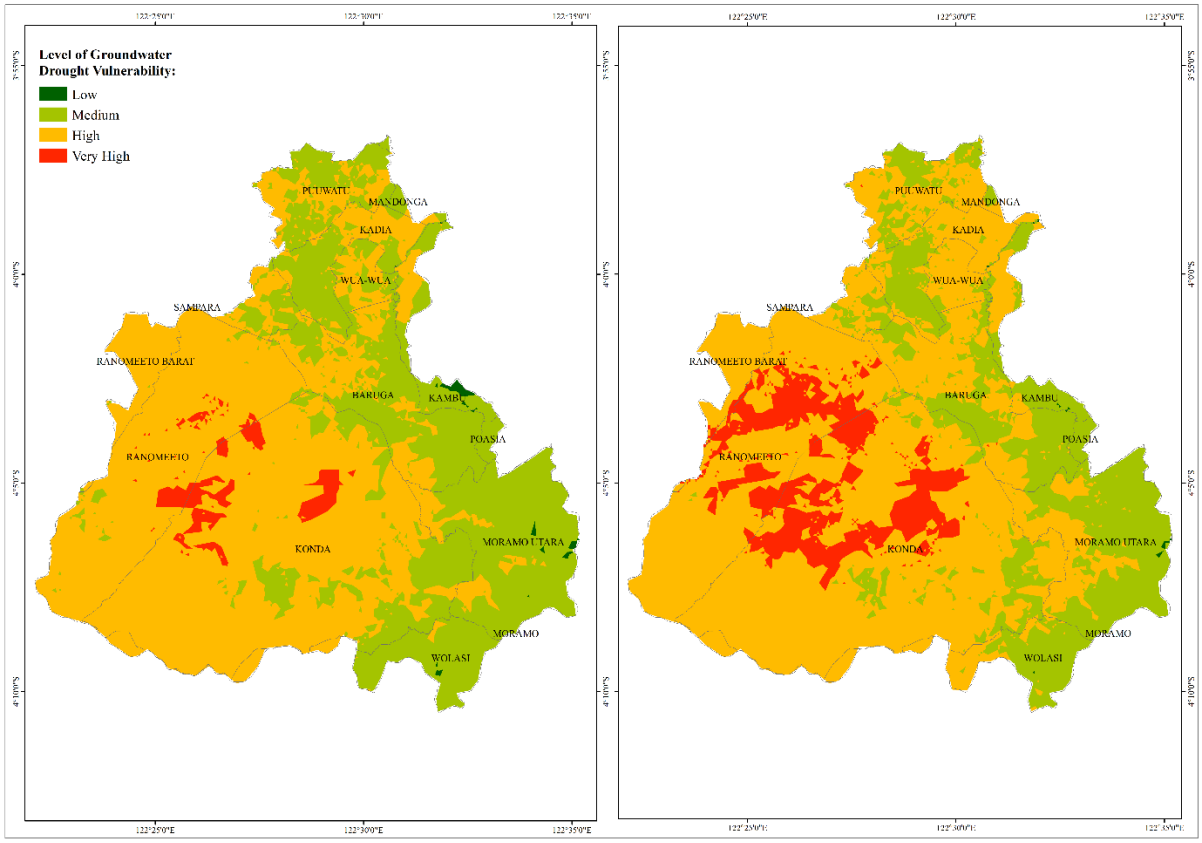

(a) (b)

Figure 7. Projection of groundwater drought vulnerability under different climate scenarios (a) Shared Socioeconomic Pathways (SSP2-45), (b) Shared Socioeconomic Pathways (SSP5-85)

Figure 7 depicts the distribution of groundwater drought vulnerability levels in the Wanggu catchment under two climate change conditions, SSP2-4.5 (Figure 7(a)) and SSP5-8.5 (Figure 7(b)). That future groundwater drought vulnerability remains spatially differentiated and becomes more severe under stronger climate forcing. Under SSP2-4.5, areas of high vulnerability remain relatively concentrated in the central and southwestern parts of the watershed. Under SSP5-8.5, however, these areas expand more widely toward the central and southern regions. This projected shift can be interpreted as the combined effect of hydroclimatic stress and land-use change. The projected climate conditions show spatial variation in rainfall and evapotranspiration across the watershed, while the land-use projection, as shown in Table 3, suggests a transition toward less infiltration-supporting land cover. Built-up land is projected to increase by 1,011.17 ha (18.19%) and agricultural land by 142.98 ha (3.43%), whereas forest, open land, and scrub are projected to decline. Together, these changes imply reduced recharge capacity and increasing pressure on groundwater systems.

This interpretation is consistent with the projection as presented in Figure 8; the percentage of areas classified as having very high vulnerability is projected to increase from 2.45% under historical conditions to 2.59% under SSP2-4.5 and 10.60% under SSP5-8.5 scenarios. Notably, the SSP5-8.5 scenario shows a particularly significant increase. Similarly, areas categorized as having high vulnerability are projected to rise to 64.14% under the SSP5-8.5 scenario, resulting in a corresponding reduction in areas with low vulnerability.

These findings suggest that future conditions may exacerbate groundwater drought vulnerability and highlight the urgent need for appropriate mitigation strategies. Therefore, areas projected to remain or become highly vulnerable under future scenarios should be treated as priority zones for adaptive groundwater management, including stricter control of land conversion, recharge enhancement, improved water-use efficiency, and scenario-based groundwater monitoring.

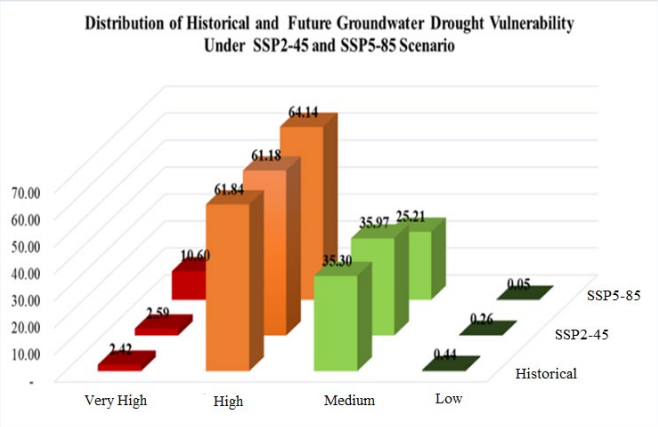

Figure 8. Distribution of groundwater drought vulnerability under historical conditions and different climate scenarios

Under SSP2-4.5, increased rainfall will also alleviate increased evapotranspiration, leading to stable groundwater recharge. Conversely, under SSP5-8.5, increased evapotranspiration surpasses increased rainfall, leading to low soil and groundwater recharge rates [9, 89].

The combined effects of land-use change and climate change can intensify groundwater drought by altering groundwater balance and reducing recharge. In particular, the conversion of vegetated land into built-up and agricultural areas may accelerate the transition from meteorological drought to hydrological drought, as built-up expansion increases impermeable surfaces and limits infiltration, while agricultural expansion raises irrigation demand, and deforestation further weakens recharge capacity. Together, these changes can lower groundwater recharge and groundwater levels, thereby increasing drought risk and overall vulnerability [89-95].

Similar results have been documented in other regions of Southeast Asia, such as Ho Chi Minh City, where rapid urbanization is predicted to substantially lower groundwater recharge as vegetated land is converted to urban built-up areas [96]. Changes to land use in the Jinjiang Coastal Catchment, China, have also substantially fragmented the recharge and runoff redistribution, whereby the expansion of built-up areas shifts the balance by increasing surface runoff and reducing infiltration to underlying aquifers [92].

Therefore, land use planning, vegetation conservation, and climate adaptation measures must be combined to ensure the hydrological resilience of the Wanggu watershed is maintained in the future. Mitigation activities and groundwater conservation not only play a major role in the conservation of groundwater but also in the proper support of food security, economic, and social sustainability. To sum up, it can be pointed out that land use trends and climate are the two big factors that have a major impact on the vulnerability to drought of groundwater in the Wanggu watershed. Changes in land use that result in decreased infiltration rates, together with increased temperature and evapotranspiration due to climate change, are the main factors that lead to a reduction of a watershed's capacity to maintain its groundwater; thus, drought vulnerability in groundwater will increase over the next several decades.

4. CONCLUSIONS

The Wanggu Watershed is an important source of freshwater for domestic, agricultural, and industrial uses, but it is increasingly exposed to groundwater drought risk. The GDVI assessment shows that more than half of the watershed currently falls within the medium to very high vulnerability classes, reflecting the combined influence of groundwater dependence, geohydrological conditions, land use, and climatological stress. Future projections to 2050 indicate that groundwater drought vulnerability is likely to intensify under both SSP2-4.5 and SSP5-8.5 scenarios, with a substantial expansion of areas classified as high to very high vulnerability, especially under SSP5-8.5. This increase is associated with the combined effects of land-use change and hydroclimatic stress, particularly higher evapotranspiration relative to rainfall. These findings suggest that groundwater management in the Wanggu Watershed should prioritize recharge protection, control of groundwater abstraction, and adaptive land-use planning. Practical measures may include infiltration wells, biopores, protection of remaining recharge areas, and vegetation restoration where feasible. Their implementation should be adapted to local conditions and supported by community participation, local regulations, and coordination among relevant stakeholders.

ACKNOWLEDGMENT

This work was supported by DRTPM-Kemendikbudristek 2025 under the Regular Fundamental Research Scheme, led by La Baco Sudia (Contract No. 36/UN29.20/PG/2025).

Special appreciation is also extended to the Rector of Halu Oleo University (UHO) and the Dean of the Faculty of Forestry and Environmental Sciences, Halu Oleo University, for their institutional support and the research facilities that made this study possible.

REFERENCES

[1] Dangar, S., Asoka, A., Mishra, V. (2021). Causes and implications of groundwater depletion in India: A review. Journal of Hydrology, 596: 126103. https://doi.org/10.1016/j.jhydrol.2021.126103

[2] Hellwig, J., De Graaf, I.E.M., Weiler, M., Stahl, K. (2020). Large-scale assessment of delayed groundwater responses to drought. Water Resources Research, 56(2): e2019WR025441. https://doi.org/10.1029/2019WR025441

[3] Wood, J.C., Wood, M.K., Tromble, J.M. (1987). Important factors influencing water infiltration and sediment production on arid lands in New Mexico. Journal of Arid Environments, 12(2): 111-118. https://doi.org/10.1016/S0140-1963(18)31181-9

[4] Mussa, M.M., Lohani, T.K., Eshete, A.A. (2025). Evaluation of the impacts of land use and land cover changes on groundwater recharge in the Gidabo watershed, Ethiopia. World Water Policy, 11(3): 751-769. https://doi.org/10.1002/wwp2.70011

[5] Cuthbert, M.O., Gleeson, T., Moosdorf, N., Befus, K.M., Schneider, A., Hartmann, J., Lehner, B. (2019). Global patterns and dynamics of climate–groundwater interactions. Nature Climate Change, 9(2): 137-141. https://doi.org/10.1038/s41558-018-0386-4

[6] Siddik, M.S., Tulip, S.S., Rahman, A., Islam, M.N., Haghighi, A.T., Mustafa, S.M.T. (2022). The impact of land use and land cover change on groundwater recharge in northwestern Bangladesh. Journal of Environmental Management, 315: 115130. https://doi.org/10.1016/j.jenvman.2022.115130

[7] Dasgupta, B., Sanyal, P. (2022). Linking land use land cover change to global groundwater storage. Science of the Total Environment, 853: 158618. https://doi.org/10.1016/j.scitotenv.2022.158618

[8] Taylor, R.G., Scanlon, B., Döll, P., et al. (2013). Ground water and climate change. Nature Climate Change, 3(4): 322-329. https://doi.org/10.1038/nclimate1744

[9] Schuler, P., Campanyà, J., Moe, H., Doherty, D., Williams, N.H., McCormack, T. (2022). Mapping the groundwater memory across Ireland: A step towards a groundwater drought susceptibility assessment. Journal of Hydrology, 612: 128277. https://doi.org/10.1016/j.jhydrol.2022.128277

[10] Romero, P., Piña, A. (2025). GRACE-based analysis of groundwater sustainability in the tropics. Journal of Hydrology: Regional Studies, 62: 102756. https://doi.org/10.1016/j.ejrh.2025.102756

[11] Gungoa, V., Kebede, S. (2024). Climate variability impact on groundwater quality in Small Island Developing States: Mauritius Island as a case study. Frontiers in Water, 6: 1432908. https://doi.org/10.3389/frwa.2024.1432908

[12] Zaki, M.K., Noda, K. (2022). A systematic review of drought indices in tropical Southeast Asia. Atmosphere, 13(5): 833. https://doi.org/10.3390/atmos13050833

[13] Nauditt, A., Stahl, K., Rodríguez, E., Birkel, C., Formiga-Johnsson, R.M., Kallio, M., Ribbe, L., Baez-Villanueva, O.M., Thurner, J., Hann, H. (2022). Evaluating tropical drought risk by combining open-access gridded vulnerability and hazard data products. Science of the Total Environment, 822: 153493. https://doi.org/10.1016/j.scitotenv.2022.153493

[14] Ling, Z., Shu, L., Wang, D., Lu, C., Liu, B. (2023). Assessment and projection of the groundwater drought vulnerability under different climate scenarios and land use changes in the Sanjiang Plain, China. Journal of Hydrology: Regional Studies, 49: 101498. https://doi.org/10.1016/j.ejrh.2023.101498

[15] FAO, Drought portal - Knowledge resources on integrated drought management, fao.org. https://www.fao.org/in-action/drought-portal/home/1/en, accessed on Oct. 29, 2025.

[16] Młyński, D., Wałęga, A., Kuriqi, A. (2021). Influence of meteorological drought on environmental flows in mountain catchments. Ecological Indicators, 133: 108460. https://doi.org/10.1016/j.ecolind.2021.108460

[17] Zhou, Z., Shi, H., Fu, Q., Ding, Y., Li, T., Liu, S. (2021). Investigating the propagation from meteorological to hydrological drought by introducing the nonlinear dependence with directed information transfer index. Water Resources Research, 57(8): e2021WR030028. https://doi.org/10.1029/2021WR030028

[18] Yu, C., Huang, X., Chen, H., Huang, G., Ni, S., Wright, J.S., Hall, J., Ciais, P., Zhang, J., Xiao, Y., Sun, Z., Wang, X., Yu, L. (2018). Assessing the impacts of extreme agricultural droughts in China under climate and socioeconomic changes. Earth's Future, 6(5): 689-703. https://doi.org/10.1002/2017EF000768

[19] Wang, J., Liu, W., Yin, D. (2025). Impacts of integrated meteorological and agricultural drought on global maize yields. Agricultural Water Management, 318: 109727. https://doi.org/10.1016/j.agwat.2025.109727

[20] Gumus, V. (2023). Evaluating the effect of the SPI and SPEI methods on drought monitoring over Turkey. Journal of Hydrology, 626: 130386. https://doi.org/10.1016/j.jhydrol.2023.130386

[21] Alam, N. M., Sharma, G.C., Moreira, E., Jana, C., Mishra, P.K., Sharma, N.K., Mandal, D. (2017). Evaluation of drought using SPEI drought class transitions and log-linear models for different agro-ecological regions of India. Physics and Chemistry of the Earth, Parts a/b/c, 100: 31-43. https://doi.org/10.1016/j.pce.2017.02.008

[22] Tsesmelis, D.E., Vasilakou, C.G., Kalogeropoulos, K., Stathopoulos, N., Alexandris, S.G., Zervas, E., Oikonomou, P.D., Karavitis, C.A. (2022). Drought assessment using the standardized precipitation index (SPI) in GIS environment in Greece. Computers in Earth and Environmental Sciences, 2022: 619-633. https://doi.org/10.1016/B978-0-323-89861-4.00025-7

[23] Ajaz, A., Taghvaeian, S., Khand, K., Gowda, P.H., Moorhead, J.E. (2019). Development and evaluation of an agricultural drought index by harnessing soil moisture and weather data. Water, 11(7): 1375. https://doi.org/10.3390/w11071375

[24] Luan, Q., Gu, P., Sun, Q., Lai, B., Zhou, Y., Weng, B. (2024). Agricultural drought evaluation based on a soil moisture index coupled hydrological model in North China Plain. Ecological Indicators, 166: 112473. https://doi.org/10.1016/j.ecolind.2024.112473
[25] Nalbantis, I. (2008). Evaluation of a hydrological drought index. European Water, 23(24): 67-77.
[26] Block, P.J., Souza Filho, F.A., Sun, L., Kwon, H.H. (2009). A streamflow forecasting framework using multiple climate and hydrological models 1. JAWRA Journal of the American Water Resources Association, 45(4): 828-843. https://doi.org/10.1111/J.1752-1688.2009.00327.X
[27] Goswami, G., Prasad, R.K., Mandal, S. (2025). Streamflow variability under SSP2-4.5 and SSP5-8.5 climate scenarios using QSWAT plus for Subansiri River Basin in Arunachal Pradesh, India. Theoretical and Applied Climatology, 156(5): 260. https://doi.org/10.1007/s00704-025-05496-x
[28] Wang, F., Wang, Z., Yang, H., Di, D., Zhao, Y., Liang, Q., Hussain, Z. (2020). Comprehensive evaluation of hydrological drought and its relationships with meteorological drought in the Yellow River basin, China. Journal of Hydrology, 584: 124751. https://doi.org/10.1016/j.jhydrol.2020.124751
[29] Apsari, B.S., Fitriani, V., Yuristiawan, S.T. (2026). Distribution of meteorological drought and its implications in Jember Regency. Majalah Geografi Indonesia, 40(1): 67-73. https://doi.org/10.22146/mgi.108615
[30] Liu, Y., Shan, F., Yue, H., Wang, X., Fan, Y. (2023). Global analysis of the correlation and propagation among meteorological, agricultural, surface water, and groundwater droughts. Journal of Environmental Management, 333: 117460. https://doi.org/10.1016/j.jenvman.2023.117460
[31] Alwi, L., Sinukaban, N., Salahuddin, S., Pawitan, H. (2011). Study of the dynamic impact on land erosion and hydrological conditions in the Wanggu watershed. Journal Hidrolitan, 2: 74-86.
[32] Marwah, S. (2015). Analysis of the impact of land use changes on land degradation and farmer income in the Wanggu Watershed, Southeast Sulawesi. Jurnal Pengkajian dan Pengembangan Teknologi Pertanian, 18(2): 117-130. https://www.neliti.com/publications/139362/analisis-dampak-perubahan-penggunaan-lahan-terhadap-degradasi-lahan-dan-pendapat#cite.
[33] BPK Regulation Database. (2006). Regulation of the Minister of Home Affairs Number 23 of 2006 concerning Technical Guidelines and Procedures for Regulating Drinking Water Tariffs at Regional Drinking Water Companies. https://peraturan.bpk.go.id/Details/126458/permendagri-no-23-tahun-2006.
[34] Doorenbos, J., Pruitt, W.O. (1977). FAO irrigation and drainage paper No. 24: Guidelines for predicting crop water requirements. Food and Agriculture Organization of the United Nations, 1977. https://www.fao.org/4/f2430e/f2430e.pdf.
[35] Melo, G.L.D., Fernandes, A.L. (2012). Evaluation of empirical methods to estimate reference evapotranspiration in Uberaba, State of Minas Gerais, Brazil. Engenharia Agrícola, 32: 875-888. https://doi.org/10.29303/jrpb.v12i2.629
[36] Alwi, L.O., Gandri, L. (2020). Analysis of policy priority in conservation of water resources on various types of land uses (case of flood prevention models in Kendari city). Research Inventy: International Journal of Engineering and Science, 10(8): 1-10.
[37] Erdogan, S.A., Šaparauskas, J., Turskis, Z. (2017). Decision-making in construction management: AHP and expert choice approach. Procedia Engineering, 172: 270-276. https://doi.org/10.1016/j.proeng.2017.02.111
[38] Ishizaka, A., Labib, A. (2009). Analytic hierarchy process and expert choice: Benefits and limitations. OR Insight, 22(4): 201-220. https://doi.org/10.1057/ori.2009.10
[39] Yuan, W., Wang, Z., Zhang, T., Liu, Z., Ma, Y., Xiong, Y., An, F. (2024). Assessment and prediction of groundwater vulnerability based on land use change—A case study of the central urban area of Zhengzhou. Water, 16(24): 3716. https://doi.org/10.3390/w16243716
[40] Liu, X., Liang, X., Li, X., Xu, X., Ou, J., Chen, Y., Li, S., Wang, S., Pei, F. (2017). A future land use simulation model (FLUS) for simulating multiple land use scenarios by coupling human and natural effects. Landscape and Urban Planning, 168: 94-116. https://doi.org/10.1016/j.landurbplan.2017.09.019
[41] Hu, Y., Raza, A., Syed, N.R., Acharki, S., Ray, R.L., Hussain, S., Dehghanisanij, H., Zubair, M., Elbeltagi, A. (2023). Land use/land cover change detection and NDVI estimation in Pakistan's Southern Punjab Province. Sustainability, 15(4): 3572. https://doi.org/10.3390/su15043572
[42] Tahir, Z., Haseeb, M., Mahmood, S.A., Batool, S., Abdullah-Al-Wadud, M., Ullah, S., Tariq, A. (2025). Predicting land use and land cover changes for sustainable land management using CA-Markov modelling and GIS techniques. Scientific Reports, 15(1): 3271. https://doi.org/10.1038/s41598-025-87796-w
[43] Cruz-González, A., Arteaga-Ramírez, R., Soria-Ruiz, J., Sánchez-Cohen, I., Monterroso-Rivas, A.I., Quevedo-Nolasco, A. (2025). Climate change projections in temperature and precipitation using CMIP6 in Central Mexico. Theoretical and Applied Climatology, 156(2): 97. https://doi.org/10.1007/s00704-024-05345-3
[44] Ozbuldu, M., Irvem, A. (2025). Projecting and downscaling future temperature and precipitation based on CMIP6 models using machine learning in hatay province, Türkiye. Pure and Applied Geophysics, 182(4): 1825-1842. https://doi.org/10.1007/s00024-024-03656-0
[45] Eyring, V., Bony, S., Meehl, G.A., Senior, C.A., Stevens, B., Stouffer, R.J., Taylor, K.E. (2016). Overview of the Coupled Model Intercomparison Project Phase 6 (CMIP6) experimental design and organization. Geoscientific Model Development, 9(5): 1937-1958. https://doi.org/10.5194/gmd-9-1937-2016
[46] Safura, A.H., Sekaranom, A.B. (2024). Projections of future meteorological drought in Java-Nusa Tenggara region based on CMIP6 scenario. Geographia Technica, 19(1): 43-60. https://doi.org/10.21163/GT_2024.191.04
[47] Lovato, T., Peano, D., Butenschön, M., Materia, S., Iovino, D., Scoccimarro, E., Fogli, P.G., Cherchi, A., Bellucci, A., Gualdi, S., Masina, S., Navarra, A. (2022). CMIP6 simulations with the CMCC Earth system model (CMCC-ESM2). Journal of Advances in Modeling Earth Systems, 14(3): e2021MS002814.

https://doi.org/10.1029/2021MS002814
[48] Schroeter, S., Bi, D., Law, R.M., Loughran, T.F., Rashid, H.A., Wang, Z. (2024). Global-scale future climate projections from ACCESS model contributions to CMIP6. Journal of Southern Hemisphere Earth Systems Science, 74(2): ES23029. https://doi.org/10.1071/ES23029
[49] Calvin, K., Dasgupta, D., Krinner, G., et al. (2023). IPCC, 2023: Climate Change 2023: Synthesis Report. Contribution of Working Groups I, II and III to the Sixth Assessment Report of the Intergovernmental Panel on Climate Change. IPCC, Geneva, Switzerland. http://doi.org/10.59327/ipcc/ar6-9789291691647
[50] Fan, X., Miao, C., Wu, Y., Mishra, V., Chai, Y. (2024). Comparative assessment of dry-and humid-heat extremes in a warming climate: Frequency, intensity, and seasonal timing. Weather and Climate Extremes, 45: 100698. https://doi.org/10.1016/j.wace.2024.100698
[51] Su, B., Huang, J., Mondal, S. K., Zhai, J., Wang, Y., Wen, S., Gao, M., Lv, Y., Jiang, S., Jiang, T., Li, A. (2021). Insight from CMIP6 SSP-RCP scenarios for future drought characteristics in China. Atmospheric Research, 250: 105375. https://doi.org/10.1016/j.atmosres.2020.105375
[52] Humphries, U.W., Waqas, M., Hlaing, P.T., Dechpichai, P., Wangwongchai, A. (2024). Assessment of CMIP6 GCMs for selecting a suitable climate model for precipitation projections in Southern Thailand. Results in Engineering, 23: 102417. https://doi.org/10.1016/j.rineng.2024.102417
[53] Beyer, R., Krapp, M., Manica, A. (2020). An empirical evaluation of bias correction methods for palaeoclimate simulations. Climate of the Past, 16(4): 1493-1508. https://doi.org/10.5194/cp-16-1493-2020
[54] Gebresellase, S.H., Wu, Z., Xu, H., Muhammad, W.I. (2022). Evaluation and selection of CMIP6 climate models in Upper Awash Basin (UBA), Ethiopia: Evaluation and selection of CMIP6 climate models in Upper Awash Basin (UBA), Ethiopia. Theoretical and Applied Climatology, 149(3): 1521-1547. https://doi.org/10.1007/s00704-022-04056-x
[55] Muñoz Sabater, J. (2019). ERA5-Land hourly data from 1981 to present. Copernicus Climate Change Service (C3S) Climate Data Store (CDS), 10(10.24381). https://doi.org/10.24381/cds.e2161bac
[56] Funk, C., Peterson, P., Landsfeld, M., Pedreros, D., Verdin, J., Shukla, S., Husak, G., Rowland, J., Harrison, L., Hoell, A., Michaelsen, J. (2015). The climate hazards infrared precipitation with stations—A new environmental record for monitoring extremes. Scientific Data, 2(1): 150066. https://doi.org/10.1038/sdata.2015.66
[57] Ershadfath, F., Davarpanah, R., Sa'adi, Z., Piniewski, M., Trolle, D., Olesen, J.E. (2025). Selecting CMIP6 precipitation models by integrating relative importance metrics, compromise programming index, and Jenks optimized classification. Science of the Total Environment, 1006: 180935. https://doi.org/10.1016/j.scitotenv.2025.180935
[58] Paredes, P., Pereira, L.S., Almorox, J., Darouich, H. (2020). Reference grass evapotranspiration with reduced data sets: Parameterization of the FAO Penman-Monteith temperature approach and the Hargreaves-Samani equation using local climatic variables. Agricultural Water Management, 240: 106210. https://doi.org/10.1016/j.agwat.2020.106210
[59] Maraun, D., Shepherd, T.G., Widmann, M., Zappa, G., Walton, D., Gutiérrez, J.M., Hagemann, S., Richter, I., Soares, P.M.M., Hall, A., Mearns, L.O. (2017). Towards process-informed bias correction of climate change simulations. Nature Climate Change, 7(11): 764-773. https://doi.org/10.1038/nclimate3418
[60] Lafferty, D.C., Sriver, R.L. (2023). Downscaling and bias correction contribute considerable uncertainty to local climate projections in CMIP6. NPJ Climate and Atmospheric Science, 6(1): 158. https://doi.org/10.1038/s41612-023-00486-0
[61] Navarro-Racines, C., Tarapues, J., Thornton, P., Jarvis, A., Ramirez-Villegas, J. (2020). High-resolution and bias-corrected CMIP5 projections for climate change impact assessments. Scientific Data, 7(1): 7. https://doi.org/10.1038/s41597-019-0343-8
[62] Oruc, S. (2022). Performance of bias-corrected monthly CMIP6 climate projections with different reference period data in Turkey. Acta Geophysica, 70(2): 777-789. https://doi.org/10.1007/s11600-022-00731-9
[63] Räty, O., Räisänen, J., Ylhäisi, J.S. (2014). Evaluation of delta change and bias correction methods for future daily precipitation: Intermodel cross-validation using ENSEMBLES simulations. Climate Dynamics, 42(9): 2287-2303. https://doi.org/10.1007/s00382-014-2130-8
[64] Timbrell, L., Blinkhorn, J., Colucci, M., Leonardi, M., Chevalier, M., Pozzi, A.V., Grove, M., Scerri, E., Manica, A. (2025). More is not always better: Delta-downscaling climate model outputs from 30 to 5 min resolution has minimal impact on coherence with Late Quaternary proxies. Climate of the Past, 21(7): 1185-1208. https://doi.org/10.5194/cp-21-1185-2025
[65] Lite, S.J., Bagstad, K.J., Stromberg, J.C. (2005). Riparian plant species richness along lateral and longitudinal gradients of water stress and flood disturbance, San Pedro River, Arizona, USA. Journal of Arid Environments, 63(4): 785-813. https://doi.org/10.1016/j.jaridenv.2005.03.026
[66] Tsheboeng, G. (2018). Spatial variation of the influence of distance from surface water on riparian plant communities in the Okavango Delta, Botswana. Ecological Processes, 7(1): 32. https://doi.org/10.1186/s13717-018-0140-x
[67] Foster, S.S.D., Chilton, P.J. (2003). Groundwater: The processes and global significance of aquifer degradation. Philosophical Transactions of the Royal Society of London. Series B: Biological Sciences, 358(1440): 1957-1972. https://doi.org/10.1098/rstb.2003.1380
[68] Stromberg, J.C., Tiller, R., Richter, B. (1996). Effects of groundwater decline on riparian vegetation of semiarid regions: The San Pedro, Arizona. Ecological Applications, 6(1): 113-131. https://doi.org/10.2307/2269558
[69] Lerner, D.N., Harris, B. (2009). The relationship between land use and groundwater resources and quality. Land Use Policy, 26: S265-S273. https://doi.org/10.1016/j.landusepol.2009.09.005
[70] Kintoro, F.S., Adji, T.N., Widyastuti, M. (2025). Land use changes and their impact on groundwater vulnerability's spatio-temporal conditions. Journal of Degraded and Mining Lands Management, 12(2): 6979-6990. https://doi.org/10.15243/jdmlm.2025.122.6979

[71] Garg, K.K., Anantha, K.H., Nune, R., Akuraju, V.R., Singh, P., Gumma, M.K., Dixit, S., Ragab, R. (2020). Impact of land use changes and management practices on groundwater resources in Kolar district, Southern India. Journal of Hydrology: Regional Studies, 31: 100732. https://doi.org/10.1016/j.ejrh.2020.100732

[72] Birylo, M. (2020). Elaboration of the relationship between the groundwater level in unconfined aquifer and the value of precipitation and evapotranspiration. Environmental Sciences Proceedings, 2(1): 17. https://doi.org/10.3390/environsciproc2020002017

[73] Yang, H., Yoo, H., Lim, H., Kim, J., Choi, H.T. (2021). Impacts of soil properties, topography, and environmental features on soil water holding capacities (SWHCs) and their interrelationships. Land, 10(12): 1290. https://doi.org/10.3390/land10121290

[74] Hou, X., Yang, H., Cao, J., Feng, W., Zhang, Y. (2023). A review of advances in groundwater evapotranspiration research. Water, 15(5): 969. https://doi.org/10.3390/w15050969

[75] Diouf, O.C., Weihermüller, L., Diedhiou, M., Vereecken, H., Faye, S.C., Faye, S., Sylla, S.N. (2020). Modelling groundwater evapotranspiration in a shallow aquifer in a semi-arid environment. Journal of Hydrology, 587: 124967. https://doi.org/10.1016/j.jhydrol.2020.124967

[76] BMKG. (2023). Climate Variability. https://iklim.bmkg.go.id/bmkgadmin/storage/brosur/LEAFLETINDO.pdf.

[77] Richey, A.S., Thomas, B.F., Lo, M.H., Reager, J.T., Famiglietti, J.S., Voss, K., Swenson, S., Rodell, M. (2015). Quantifying renewable groundwater stress with GRACE. Water Resources Research, 51(7): 5217-5238. https://doi.org/10.1002/2015WR017349

[78] Wada, Y., Van Beek, L.P., Van Kempen, C.M., Reckman, J.W., Vasak, S., Bierkens, M.F. (2010). Global depletion of groundwater resources. Geophysical Research Letters, 37(20): L20402. https://doi.org/10.1029/2010GL044571

[79] Winter, T.C., Harvey, J.W., Franke, O.L., Alley, W.M. (1998). Ground water and surface water: A single resource. Circular. https://doi.org/10.3133/cir1139

[80] Perrone, D., Jasechko, S. (2019). Deeper well drilling an unsustainable stopgap to groundwater depletion. Nature Sustainability, 2(8): 773-782. https://doi.org/10.1038/s41893-019-0325-z

[81] Greve, P., Orlowsky, B., Mueller, B., Sheffield, J., Reichstein, M., Seneviratne, S.I. (2014). Global assessment of trends in wetting and drying over land. Nature Geoscience, 7(10): 716-721. https://doi.org/10.1038/ngeo2247

[82] Scanlon, B.R., Healy, R.W., Cook, P.G. (2002). Choosing appropriate techniques for quantifying groundwater recharge. Hydrogeology Journal, 10(1): 18-39. https://doi.org/10.1007/s10040-001-0176-2

[83] Zhao, Z., Liu, C., Yan, M., Pan, G. (2023). Understanding and enhancing soil conservation of water and life. Soil Science and Environment, 2(1): 9. https://doi.org/10.48130/SSE-2023-0009

[84] Riaz, A., Nijhuis, S., Bobbink, I. (2025). The role of spatial planning in landscape-based groundwater recharge: A systematic literature review. Water, 17(6): 862. https://doi.org/10.3390/w17060862

[85] Zhang, K., Chui, T.F.M. (2019). A review on implementing infiltration-based green infrastructure in shallow groundwater environments: Challenges, approaches, and progress. Journal of Hydrology, 579: 124089. https://doi.org/10.1016/j.jhydrol.2019.124089

[86] Brunner, N., Starkl, M., Sakthivel, P., Elango, L., Amirthalingam, S., Pratap, C.E., Thirunavukkarasu, M., Parimalarenganayaki, S. (2014). Policy preferences about managed aquifer recharge for securing sustainable water supply to Chennai city, India. Water, 6(12): 3739-3757. https://doi.org/10.3390/w6123739

[87] Chen, P., Zhang, X., Li, E., Han, S. (2025). Analyzing the impact of land use changes on hydrological drought in the yiluo river basin based on SWAT. Environmental and Sustainability Indicators, 28: 101052. https://doi.org/10.1016/j.indic.2025.101052

[88] Adam, M.A., Scheiber-Enslin, S.E., Ali, K.A. (2025). Estimating water storage change from GRACE satellite data over the breede water management area, western cape, South Africa. Hydrogeology Journal, 33(8): 2041-2055. https://doi.org/10.1007/s10040-025-02946-8

[89] Turkeltaub, T., Bel, G. (2024). Changes in mean evapotranspiration dominate groundwater recharge in semi-arid regions. Hydrology and Earth System Sciences, 28(18): 4263-4274. https://doi.org/10.5194/hess-28-4263-2024

[90] Dai, M., Feng, P., Li, J., Shi, X., Wang, H. (2025). Effects of land use/cover change on propagation dynamics from meteorological to soil moisture drought considering nonstationarity. Agricultural Water Management, 312: 109452. https://doi.org/10.1016/j.agwat.2025.109452

[91] Yadav, D., Kumar, R., Yadav, V., Laha, A. (2025). The Fundamentals of Soil Science. P.K. Publishers & Distributors, Delhi-110053 (India).

[92] Lin, B., Chen, X., Yao, H., Chen, Y., Liu, M., Gao, L., James, A. (2015). Analyses of landuse change impacts on catchment runoff using different time indicators based on SWAT model. Ecological Indicators, 58: 55-63. https://doi.org/10.1016/j.ecolind.2015.05.031

[93] Mensah, J.K., Ofosu, E.A., Yidana, S.M., Akpoti, K., Kabo-bah, A.T. (2022). Integrated modeling of hydrological processes and groundwater recharge based on land use land cover, and climate changes: A systematic review. Environmental Advances, 8: 100224. https://doi.org/10.1016/j.envadv.2022.100224

[94] Wldmchel, M., Osore, A. (2025). Evaluation of the impact of climate and land use/land cover change on hydrological response in Gelna watershed. PLOS Climate, 4(1): e0000483. https://doi.org/10.1371/journal.pclm.0000483

[95] Riazi, M., Khosravi, K., Samani, M.R., Han, S., Eslamian, S. (2024). Assessing groundwater drought vulnerability through baseflow separation and index-based analysis under climate change projections. Groundwater for Sustainable Development, 25: 101179. https://doi.org/10.1016/j.gsd.2024.101179

[96] Yadav, S.K. (2023). Land cover change and its impact on groundwater resources: Findings and recommendations. In Groundwater-New Advances and Challenges. IntechOpen. https://doi.org/10.5772/intechopen.11031